

# The Galactic IMF: origin in the combined mass distribution functions of dust grains and gas clouds

E. Casuso<sup>(1,3)\*</sup> and J. E. Beckman<sup>(1,2,3)\*</sup>

<sup>1</sup>*Instituto de Astrofísica de Canarias, 38205, La Laguna, Tenerife, Spain*

<sup>2</sup>*C.S.I.C., Madrid, Spain*

<sup>3</sup>*Department of Astrophysics, University of La Laguna, Tenerife, Spain*

Accepted . Received ; in original form

## ABSTRACT

We present here a theoretical model to account for the stellar IMF as a result of the composite behaviour of the gas and dust distribution functions. Each of these has previously been modelled and the models tested against observations. The model presented here implies a relation between the characteristic size of the dust grains and the characteristic final mass of the stars formed within the clouds containing the grains, folded with the relation between the mass of a gas cloud and the characteristic mass of the stars formed within it. The physical effects of dust grain size are due to equilibrium relations between the efficiency of grains in cooling the clouds, which is a falling function of grain size, and the efficiency of grains in catalyzing the production of molecular hydrogen, which is a rising function of grain size. We show that folding in the effects of grain distribution can yield a reasonable quantitative account of the IMF, while gas cloud mass function alone cannot do so.

**Key words:** ISM: dust, extinction

## 1 INTRODUCTION

When we observe the mass distribution function of stars in a galaxy we obtain the present day mass function (PDMF) which is not the mass function of stars at their birth (the initial mass function, IMF) but the distribution resulting from the accumulation of stars since the first star formation occurred in the Galaxy. In this process, whether the star formation is continuous or sporadic, the most massive stars with their short lifetimes are more quickly eliminated, and the masses of all the stars are reduced secularly by mass loss, while the stellar population may be augmented by the arrival of stars from outside the Galaxy in accretion events with dwarf galaxies. The local IMF is a basic function in the study of the chemical evolution of our Galaxy, as it is the measure of the number of stars formed in a given mass interval in the solar neighborhood (Scalo 1978, 1986; Tinsley 1980). The origin of the IMF is a fundamental problem in the whole of astrophysics because it determines the photometric properties of galaxies, and the dynamical and chemical evolution of their interstellar media. Salpeter (1955) was the first to note that there appears to be a power-law relationship between the number of stars observed in the Galactic field and their masses, and it was his work which gave rise to our concept of the IMF.

In order to try to account for the form of the IMF one needs to know the mechanism of the process of star formation. We understand that this process begins with the formation of giant molecular clouds within which, given the right conditions of temperature and density (the Jeans conditions Jeans (1902)) local gravitational collapse gives rise to stars. It is also well understood that the presence of dust grains as catalysts is an essential condition for the conversion of atomic to molecular hydrogen, so that they are necessary for the presence of the giant molecular clouds. It thus appears reasonable that in order to investigate the factors which explain the stellar IMF one needs to take into account not only the gas cloud mass distribution function, but also the distribution function of the dust grain sizes. The relationship between the gas and star formation is obvious since stars form from the gas clouds, but the connection between the dust and star formation is less direct. As we have just noted, the presence of dust, even in small quantities, makes a major difference to the conversion rate of atomic to molecular hydrogen Schaye (2004), but dust also affects the heating cycle in the ISM, which affects the tendency to form the cold dense clouds needed for star formation.

Arguments based on gravitational instability and on observations of molecular gas reveal that the low-temperature ( $T \sim 10$  K) high-density ( $n \geq 40 \text{ cm}^{-3}$ ) cores in giant molecular clouds (GMC's) are the natural sites for stars to form. Although individual GMC's are well resolved in the Milky

\* E-mail: eca@iac.es

Way and in our local group (Bolatto et al. (2008), and references therein), it is from CO observations of nearby spirals which show most clearly that star formation occurs in regions dominated by molecular gas (Wong & Blitz 2002; Kennicutt et al. 2007; Bigiel et al. 2008).

The present article, whose aim is to bring out the connection between cloud mass distributions, dust grain size distributions, and the stellar mass distribution, is organized as follows: in Section 2 we present the version we will be using of the stellar IMF derived from published observations by a number of authors, in Section 3 we develop three models in which the observed mass functions for the Giant Molecular Clouds in the Galaxy will be used, in conjunction with the interstellar dust grain size distribution, to predict the IMF: the zero model (which we will combine with the three models of gas clouds to obtain the IMF) is our numerically derived dust grain size distribution function taken from Casuso & Beckman (2010) (CB10) which fits well the observed carbonate and silicate distributions, and takes into account both the production and the destruction of grains, the latter by grain-grain collisions in the ISM. The first model uses the numerically derived molecular cloud mass distribution function, taken from Casuso & Beckman (2007) (CB07) in which clouds may coagulate to form bigger clouds or may be disrupted in collisions, depending on their masses, temperatures, densities and relative velocities, while a fraction condense to form stars. The second model uses an analytically derived molecular cloud mass distribution function taken from Casuso & Beckman (2002) (CB02) where we solve the stochastic differential Langevin equation in a context of existing barriers due to box-effect. The third model uses a fully analytic approximation based on the assumption of balance between the thermal emission by dust and dust heating due to collisions with gas molecules, and is based on the CB02 approximation, in Section 4 we compare the predictions of the models with the observationally derived IMF taken from several authors, and in Section 5 we present our conclusions.

## 2 THE OBSERVATIONALLY DERIVED IMF'S

As the observational references required to test our models we have used three observational studies of the local stellar mass distribution at birth (i.e. the IMF). The first reference is Maciel & Rocha-Pinto (1998) who derive two possible IMF's, one of which assumes a constant star formation rate (SFR) and the other assumes a variable SFR derived from observations of late-type stellar populations on the main sequence. Both of these versions of the IMF used the present day stellar mass function (PDMF) by Kroupa et al. (1993). We have plotted these in Fig. 1, where we can see the difference in the slopes of the two curves due to the well understood trend of stars to disappear from the PDMF at a greater rate the higher the initial mass, and the different effect this produces using different histories for the SFR. The change in slope required to produce the IMF from the PDMF is greater with the variable SFR, because this includes a relatively recent observed peak in the local Galactic SFR (Maciel & Rocha-Pinto 1998; Rocha-Pinto et al. 2000).

We have used two other references for the Galactic IMF, one obtained by Kroupa (2001) which takes into account

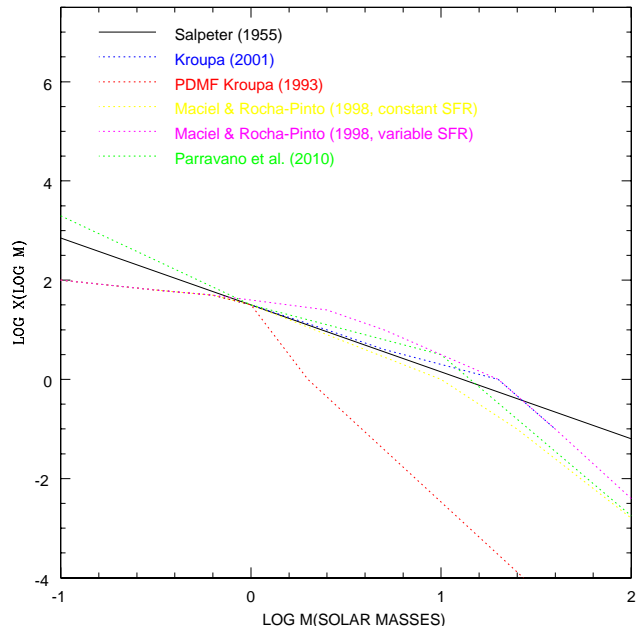


**Figure 1.** Observationally based stellar mass functions for the solar neighbourhood, compared with the classical Salpeter IMF.  $X(\log M)$  is the number of stars per logarithmic mass interval.

constraints from local star count data, and Scalo (1998) compilation of MF power law indices for young clusters and OB associations, and which shows different slopes for different mass ranges, and another, the semi-empirical Galactic IMF obtained recently by Parravano et al. (2011), both of them also shown in Fig. 1.

## 3 THE THEORETICAL MODELS, FOLDING THE GAS AND DUST DISTRIBUTION FUNCTIONS

### 3.1 Semi-analytical treatments

#### 3.1.1 The numerically derived dust grain size distribution function (GSDF)

Knowing that ISM dust grains are generally formed in the outer atmospheres of stars in the late stages of their evolution (mainly red giants, asymptotic giant branch stars, and SNe) and that grain lifetimes can be estimated as less than 100 Myr, we have taken an observational version of the local stellar birthrate to calculate the radius distribution of grains surviving today. To do so, we computed the mass distributions of stars present over this period assuming a standard IMF, the observed stellar birthrate function, and stellar lifetimes as a function of their masses, and folded in the initial distribution of dust grain sizes at each epoch, according to a simple prescription of grains produced in different stellar mass ranges. The differences between the size distribution of grains produced in the older, low mass stellar population and those produced in younger, high mass stars include the tendency of the smaller grains to be preferentially destroyed by shocks in the post-SN environment. Under these

assumptions, the major peak in the grain size distribution comes from dust produced in the younger more massive stars, and the three peaks in the interstellar dust grain size distribution function (GSDF) of carbonaceous grains correspond to the three maxima in the local SFR, as detailed in Rocha-Pinto et al. (2000). This correlation between the three main star formation events in the Galaxy and the three peaks observed for the sizes of grains appears clear. For silicates, the observed GSDF shows only one peak, close to the biggest peak in the distribution observed for carbonaceous grains. This increases the plausibility of the scenario in which the peak for carbonaceous grains at the smallest radii is associated with those grains produced during an interval of some 10 Myr near the late-stages stars of lower masses (near  $1 M_{\odot}$  arising from the earliest major peak in the SFR) because in that case the velocities of grains in the expanding shells are lower than in stars with higher masses so that the time interval for collisions among grains is greater so the probability of shattering is higher and the mean sizes of the grains are lower. For the second peak, we have grains coming from stars of intermediate age (intermediate mass coming from the second peak in the SFR) where the velocities of grains are intermediate and so some of the larger grains can escape from the high density shells where the shattering can break them into smaller grains. Finally the third peak, with the largest grains, can come from SNe where the expansion velocities are so high that the largest grains can escape from the shells into the ISM where the densities are so low that the collisions occur relatively infrequently. The observed difference in the slope of the distribution function for carbonaceous (close to 0) and silicate grains (close to 1) may be due to the mechanism proposed by Vidali et al. (2005) for suprathermal grains, whereby the misalignment with respect to the interstellar magnetic field, may be stronger for carbonaceous dust than for silicate dust. This would lead to greater collisional effects for the carbonaceous grains, changing the initial slope to that observed. The global features of the GSDF are rather well reproduced by the model in which we use only the dust sizes yielded by the stellar production process and the accompanying modifications due to shattering in the local environment of the late stages of the stars, together with a stellar birthrate function from observations. However, a closer fit to the carbonaceous grain distribution at the low radius end is obtained if we also include the modeling of longer term grain-grain collisions processes in the ISM (CB10). In Fig. 2 we can see the complete model (full line) and the comparison with data.

### 3.1.2 The numerically derived molecular cloud gas mass distribution function (MCGMF).

As one can see in CB07 we parameterize the distribution mass function of gas clouds at a given epoch as a function of their initial distributions of density, temperature, velocity, and mass. The position and velocity distributions are three-dimensional. We assume different sets of initial distribution functions, (Gaussian, flat, power-law) for temperature, densities, masses, and velocities of an initial sample of  $\sim 1000$  gas clouds, either pressure bound or gravitationally bound, evolving within a confinement volume specified as a cubic box, and arranged initially as knots in a cubic grid. Because our best fit to data is found for Gaussian distributions, and

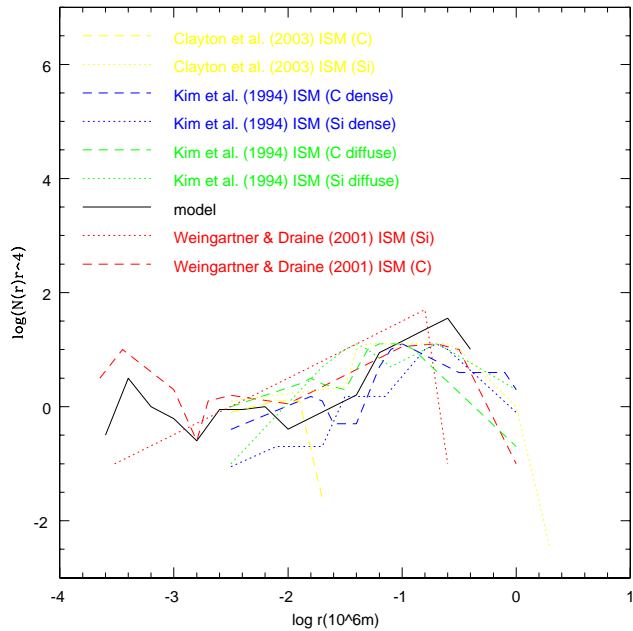


**Figure 2.** Model of the GSDF produced by combining the stellar grain production curve with the effects of size modification due to collisions in the circumstellar environment. Observational data sets are shown for comparison.

for spheroidal gas clouds we have taken that case for the present work. Each cloud has an effective volume that depends on its mass and density via  $V \simeq \frac{M}{\rho}$ . After a given evolution time, with a given initial set of velocities, we consider that two of the clouds have collided if the distance between their centers is less than or equal to the sum of their radii  $r$ , which are calculated using  $r = \left(\frac{3M}{4\pi\rho}\right)^{1/3}$ . To take particular values for the main physical parameters (density, temperature, velocity, and mass) we take the expression:

$$f(x) = \frac{1}{\sigma(2\pi)^{1/2}} e^{-\left(\frac{x-X_0}{2^{1/2}\sigma}\right)^2} \quad (1)$$

where  $f(x)$  is the probability distribution function of a variable  $X$  centred on a value  $X_0$  and with a dispersion  $\sigma$ . We have inverted these functions using the formula:

$$X = X_0 + \Delta X(-2\sigma^2 \log[f_1(x)]) \cos[2\pi f_2(x)] \quad (2)$$

where  $f_1$  and  $f_2$  are two random values of the distribution, and  $\Delta X$  is the range of values permitted for the variable  $X$ . To take into account the phenomenon of gas cloud collapse to form stars, we assume that those gas clouds that have attained the Jeans mass disappear and we count them as new stars (however, if these stars have masses big enough that their lifetimes are less than the time during which the model runs, these stars also disappear). We have taken for the Jeans mass the classical expression  $M_J = \frac{1}{6}\pi^{5/2}\rho^{-1/2}v_s^3G^{-3/2}$ , where  $\rho$  is the variable density of the gas cloud,  $v_s$  is the sound speed, and  $G$  is the gravitational constant. If  $t - t_i \geq \frac{11700}{m^2}$  then a star with mass  $m$  formed at time  $t_i$  is not computed at the current time  $t$ . The input free parameters of the model are: (1) the width and centre of the Gaussians (normalized to 1) for temperature,

velocity component (one for each of the three coordinates), mass, and density; (2) the ranges of values permitted for temperature, velocity component, mass, and density; (3) the critical values adopted for temperature, velocity and density, and of course the number of time steps considered for the time evolution. At each time step, if the temperatures of the two colliding gas clouds are greater than the adopted critical temperature, the relative velocity of the clouds is less than the critical velocity, and the densities of the two clouds are less than the critical density, i.e., the collision is completely inelastic, then we assume that one cloud disappears, while the other cloud change to a new cloud with a mass equal to the sum of the masses of the initial two clouds (the clouds merge). If all the previous conditions occur, but the relative velocity between clouds is greater than the critical velocity, then we assume that both clouds disappear by diffusion into the diffuse ISM. If the temperatures of the two clouds are less than the critical temperature, and the two densities are greater than the critical density, then we differentiate two cases: (1) when the relative velocity is less than the critical velocity, then star formation occurs and the two clouds disappear; and (2) when the relative velocity is greater than the critical velocity, we assume that each of the two clouds breaks into two subclouds, for simplicity each subcloud having half of the mass of the parent cloud. If the temperature of one cloud is less than the critical temperature and the temperature of the other is greater than the critical temperature, and the density of the first cloud is greater than the critical density while the other density is less than the critical density, then the first cloud remains unchanged, while the second cloud breaks into two subclouds each with a mass half the mass of the parent cloud. All the kinematics are computed subject to momentum conservation in each kind of collision. So for the first case, i.e., a completely inelastic collision (merger), the output velocity for each of the three dimensions is computed as  $v'_i = \frac{M_1 v_{1,i} + M_2 v_{2,i}}{M_1 + M_2}$ , where the superscripts 1 and 2 indicate each of the two colliding clouds, and the subscript  $i$  indicates each direction in space ( $x$ ,  $y$ ,  $z$ ). For the case in which each cloud breaks into two subclouds, we assume that for the four resultant subclumps, those assigned 1 and 3 have the same  $x, y$  velocity components computed via  $v'_i = \frac{2M_2 v_{2,i}}{M_1 + M_2} + \frac{(M_1 - M_2)v_{1,i}}{M_1 + M_2}$ , where  $v_{j,i}$  indicates the velocity component  $i$  of the initial cloud  $j$ , and the  $z$ -direction will be such that  $v'_{1,z} = -v'_{3,z}$ , with  $v'_{1,z} = v'_z$ . Similarly for the other two output subclumps 2 and 4, using  $v'_i = \frac{2M_1 v_{1,i}}{M_1 + M_2} - \frac{(M_1 - M_2)v_{2,i}}{M_1 + M_2}$ , and  $v'_{2,z} = -v'_{4,z}$ , with  $v'_{2,z} = v'_z$ . For the case when one cloud remains unaltered (called 1), while the other breaks into two pieces (called 2 and 3), the output velocity of cloud 1 changes to the  $v'_i = \frac{2M_2 v_{2,i}}{M_1 + M_2} + \frac{(M_1 - M_2)v_{1,i}}{M_1 + M_2}$ , while the other two components 2 and 3 have the output velocities  $v'_i = \frac{2M_1 v_{1,i}}{M_1 + M_2} - \frac{(M_1 - M_2)v_{2,i}}{M_1 + M_2}$  and  $v'_{2,z} = -v'_{3,z}$ . To simulate the fact that the clouds lie on gravitationally bound orbits, we impose box shaped boundary conditions, such that the sign of the relevant velocity component changes when the cloud reaches the edge of the box. One can see in Fig. 3 the result compared with data.

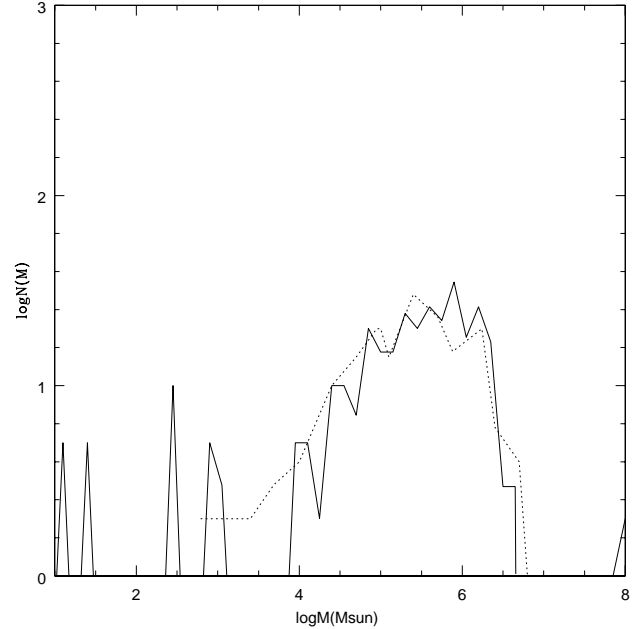


**Figure 3.** Model of the Galactic gas cloud mass distribution function, taken from CB07, (solid line) compared with observational data from Solomon et al. (1987) dotted line. The form of this function is not similar to that of the stellar IMFs shown in Fig. 1, but does play a role in determining the IMF as explained in Section 3 of this article.

### 3.1.3 The analytically derived molecular cloud gas mass distribution function.

The spaces between the gas clumps inside a cloud are large, i.e., they show a low filling factor of 0.1 for clumps within giant molecular clouds (GMCs), implying a distance between clumps of  $\sim 6$  pc while the size of each clump is typically of 1 pc. A similar structure is observed for the clouds in the galactic disk as a whole: characteristic distances between clouds are of  $5 \times 10^2$  pc while the size of a cloud is of order 10 pc. These observational data, together with the observed relative velocities:  $5 \text{ km s}^{-1}$  between clumps and  $50 \text{ km s}^{-1}$  between GMCs in the disk, permit us to make the approximation that the general distribution of gas in the ISM may be driven by random collisions leading to a Brownian (Gaussian) distribution function of displacements, at least after a sufficiently long period of time. In fact, we can see how the clumps of gas clouds have number distributions against size which in log-log plots appear as perfect Gaussian distributions (see CB02). Translated to linear units this implies Planckian distributions divided by size, implying an origin based on a system formally equivalent to standing waves in a box, although in fact somewhat more complex. As a first approximation we consider the stochastic differential Langevin equation for the time evolution of a sample of clouds under Brownian motion and also suffering the effects of a magnetic field  $B$ . Assuming that  $B$  is uniform, time independent, and perpendicular to the velocity  $u$  of clouds, for simplicity, one has:

$$\frac{du}{dt} = -\lambda u + A(t) - \frac{quB}{m} \quad (3)$$

where  $q$  and  $m$  denote the charge and mass of the cloud respectively. In this equation the influence of the surrounding medium on the cloud can be split into three terms: firstly, a systematic term  $-\lambda u$  representing a friction experienced by the cloud, due to its movement through the other clouds; second, a fluctuating term  $A(t)$  which is the characteristic of stochastic Brownian motion; and third, the simplified influence of an assumed uniform and constant magnetic field  $B$ . We have taken a magnetic force proportional to the velocity, because the magnetic force per unit volume at a distance  $R$  from the galactic centre is  $\sim \frac{B^2}{8\pi R}$ , and the magnetic flux in a galactic disk is  $\rho u \propto B^2$ . The frictional term  $-\lambda u$  is assumed to be governed by Stokes' law: the frictional force decelerating a spherical cloud of radius  $b$  and mass  $m$  is given by  $\frac{6\pi b \eta u}{m}$ , where  $\eta$  denotes the coefficient of viscosity of the surrounding fluid. Hence one has  $\lambda = \frac{6\pi b \eta}{m}$ . The fluctuating term  $A(t)$  has been restricted for simplicity to be independent of  $u$  and with variations extremely rapid compared to the variations in  $u$ . To solve equation (3) first we write it as

$$\frac{du}{dt} = -\beta u + A(t) \quad (4)$$

with

$$\beta = \lambda + \frac{qB}{m} = \frac{6\pi b \eta + qB}{m} \quad (5)$$

Now the solution to equation (4) when  $t \gg \beta^{-1}$  is:

$$W(x, t; x_0, u_0) \simeq \frac{1}{(4\pi Dt)^{1/2}} e^{-\frac{(x-x_0)^2}{4Dt}} \quad (6)$$

with  $D = \frac{kT}{6\pi b \eta + qB}$  a kind of diffusion coefficient, and  $W(x, t; x_0, u_0)$  is the probability of displacements of length  $x - x_0$  in any given direction at time  $t$  starting from initial values  $x_0$  and  $u_0$ . To obtain the same result from another physical point of view, we can consider the clouds as aggregates of microclouds. Then, the probability that a microcloud arrives at a cloud surface after a path of length  $x_1$  (assumed approximately the same as the distance between clouds) at time  $t$ , is  $P(x_1, t) = \frac{x_1}{2t(Dt\pi)^{1/2}} e^{-\frac{x_1^2}{4Dt}}$  Chandrasekhar (1943), and so, assuming that the size of microclouds is approximately constant, the distribution of sizes  $x$  for the final clouds should be  $W(x, t) \propto \int_0^x P(x_1, t) dx_1$ , i.e., a Gaussian distribution similar to equation (6). To make the change of variable from displacements  $x$  to masses  $m$ , we assume that the distribution of displacements of clouds before collision with other clouds of similar size, is comparable to that of the sizes of the clouds. This assumption, taken together with the observational relation between the sizes and masses:  $x \propto m^\alpha$  with  $0.27 \leq \alpha \leq 0.41$  leads to a distribution:

$$\frac{dN}{dm} \propto m^{\alpha-1} e^{-\frac{m^{2\alpha}}{\sigma}} \quad (7)$$

However, because the regions where the clouds move (mainly the spiral arms) are regions where the motion is limited spatially, we can treat the motion formally as if were confined within a box with walls which, although not in fact fixed, may be treated as fixed to a first approximation. And this situation can be formulated by a distribution function of displacements which is the addition of several Gaussians: the main Gaussian (centred on zero), and the other Gaussians centred on the walls which reflect the clouds whose displacements are distributed following the main Gaussian

(see CB02). Selecting the expression for a single wall and taking  $x_0 = 0$  and  $u_0 = 0$  we have:

$$W(x, t) \simeq \frac{1}{(4\pi Dt)^{1/2}} \left[ e^{-\frac{x^2}{4Dt}} + e^{-\frac{(L-x)^2}{4Dt}} \right] \quad (8)$$

where  $L/2$  is the size of the region, and the maximum of  $W(x, t)$  is at  $x_0 = L/2$ . We have neglected losses of clouds through the barrier (i.e. out of the confined region). Since  $x \propto m^\alpha$ , one can assume  $L \propto M_C^\alpha$ , and then one has the final distribution:

$$\frac{dN}{dm} \propto m^{\alpha-1} \left[ e^{-\frac{m^{2\alpha}}{\sigma}} + e^{-\frac{(M_C^\alpha - m^\alpha)^2}{\sigma}} \right] \quad (9)$$

### 3.1.4 Folding the gas and dust distribution functions.

We propose here that there is a monotonic dependence of the mass scale of stars forming within a given gas cloud, and the scale of the dust grain size within the cloud. This hypothesis has *a priori* plausibility because it is based on the known requirement of dust grain surfaces to catalyze the formation of  $H_2$  molecules from an initial cloud of HI. The fractal nature of the dust grains implies that the larger are the grains the greater is their effective catalytic surface to volume ratio, so that larger grains tend to give rise to a greater molecular fraction. There are other effects working in the same direction. Larger grains are formed, and maintained unfragmented, preferentially in regions with recent massive star formation, and as the reaction from HI to  $H_2$  proceeds more rapidly under conditions of greater hydrostatic pressure (Elmegreen 1989; Blitz & Rosolowsky 2004; Blitz et al. 2006), and supernovae arising from massive stars give periodic bursts of high pressure, these two effects combine to yield more massive molecular clouds in regions with previous high mass stellar populations. Following from this, if high mass molecular clouds yield stars with higher ranges of mass, we could expect to find a relation between dust grain size and the stellar mass range, because as we have mentioned above, lower mass stars tend to produce dust grains of lower size, which "seed" molecular clouds of lower mass, which in their turn produce a lower range of stellar masses. However there is a further effect which must be taken into account, which is that the grain distribution affects the internal radiative equilibrium of the molecular clouds and hence their tendency to condense into cores and then stars. The external radiating surfaces of the larger dust grains are proportionally smaller than those of their smaller counterparts with equal volume, so that larger clouds cool less efficiently and the Jeans masses of their cores are higher. This effect will tend to augment the tendency of the higher mass molecular clouds to yield higher ranges of stellar masses. The model we use therefore has two basic inputs: the cloud mass distribution and the grain size distribution. In our first model (model A), we have taken a numerically derived MCGMF, from section 3.1.2 and folded it with the GSDF from section 3.1.1. In order to perform this folding we normalize the distributions: we take the intervals in  $\log r(\mu m)$  between -3.6 and -0.4 for the GSDF (see Fig. 2) and identify these extremes with those of the MCGMF: 4 and 6.5 in  $\log M_\odot$  (see Fig. 3). Then we divide both intervals in 100 equal parts. So, we normalize dividing each linear value of GSDF by its higher value in the interval, and the same for MCGMF, then trans-

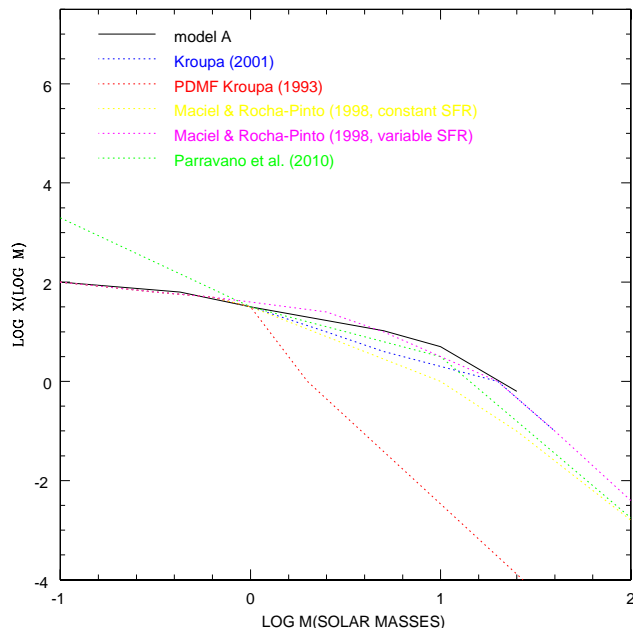


**Figure 4.** Prediction of our model A, using a numerical molecular cloud mass function (Section 3.1.2) folded with the dust grain size function (Section 3.1.1, Fig. 2), compared with three observationally based IMF's.

forming both distributions to other distributions normalized to unity in linear values. We then interpret the normalized MCGMF and GSDF as probability densities, multiplying them together point by point, and normalizing the results to 2 in  $\log X(\log M)$ . Finally, we assimilate the extremes of both intervals (that of the GSDF and that of the MCGMF) to the extremes of a new interval of stellar masses at birth taken from  $0.1 M_{\odot}$  to  $25 M_{\odot}$ . The curve we find using this semi-analytical approach, model A, is shown in Fig. 4 (full line). To explore an alternative approach we have used a theoretical model for the MCGMF, based on CB02, in which the cloud mass distribution was computed using a simplified model in which the internal cloud dynamics was determined by the interaction of gravitational bounding and turbulent gas pressure. We fold this function with the theoretical grain size distribution of CB10 as in model A and the result is our model B (full line in Fig. 5) where we have extrapolated linearly the results to  $100 M_{\odot}$ .

In the process of identification of ranges (in fact the limiting values) of cloud mass and grain size we obtain two semi-empirical relationships. We then make a linear fit to a statistically representative set of 100 values of  $\log r$  as a function of the 100 values of  $\log M_C$  and also for the 100 values of the stellar masses at birth  $\log M$  and so we obtain relations whose validity rests only on the good fits to data of the IMFs obtained from these relations (see Figs. 4 and 5). The first relation implies a functional dependence between the characteristic stellar mass,  $M$ , formed as a result of the internal collapse of a major gas cloud and the mass,  $M_C$ , of the cloud, and is just  $M_C \sim 10^5 M$ . The second is a relation between the characteristic stellar mass,  $M$ , (in units of solar mass) and the characteristic linear size,  $r$  (in  $\mu\text{m}$ ) of

the dust grains in the cloud, which is  $M \sim 25r^{0.7}$ . This trend, at least in qualitative terms, can be understood from the known requirement of grain surfaces for the catalytic conversion of HI to H<sub>2</sub> (Gould & Salpeter 1963; Cazaux & Spaans 2004; Vidali et al. 2005). This implies that the mass of a cloud should increase with grain surface available. It is also known that because of the fractal geometry of dust grains (Mutschke et al. (2009), who tested grain shape models in laboratory tests) the catalytic surface varies both with radius and with shape. Spheroidal grains have effective surfaces which increase as  $r^2$ , so their surface per unit mass falls with increasing radius, obeying an  $r^{-1}$  relation. Toroidal shapes with constant section have effective surface and volume varying as  $r^1$ , so their effective surface area per unit mass is constant, and independent of radius. Fractal grains have effective surfaces which vary with their radii according to a power law with index very different from 2, which would lead us to anticipate a possible dependence of cloud mass on grain size with a positive index, as we can infer from the result of our normalization. It is worth noting here that the effective surface area for catalytic reactions will be, for fractal grains, much larger than the effective surface area for radiative equilibrium, since a major proportion of the fractal surface radiates into the grain, and only the outermost surface radiates energy away from the grain. Essentially the area to use in radiative equilibrium calculations will be approximately that of a spherical grain with the same global radius, and will thus vary nearly as  $r^2$  even for a fractal grain.

### 3.2 Analytical treatment

Our model C is a theoretical model based on the assumption of balance between dust thermal emission and heating due to collisions with gas particles (Schneider et al. (2006)). This leads to the equilibrium equation:

$$4\sigma T_{gr}^4 \kappa_P \beta_{esc} \rho_{gr} = n_{gr} 2k(T_G - T_{gr}) n_H \sigma_{gr} \left( \frac{8kT_G}{\pi m_H} \right)^{1/2} f \quad (10)$$

where  $\sigma$  is the Stefan-Boltzmann constant,  $T_{gr}$  is the dust temperature,  $T_G$  is the gas temperature,  $\kappa_P$  is the Planck mean opacity of dust grains, per unit mass,  $\beta_{esc}$  is the photon escape probability,  $\rho_{gr}$  is the dust mass density,  $n_{gr}$  is the grain number density,  $\sigma_{gr}$  is the mean grain cross section,  $n_H$  is the hydrogen number density,  $m_H$  the mass of the hydrogen atom, and  $k$  is the Boltzman constant. The factor  $f$  takes into account the contribution to the gas-dust equilibrium of species other than hydrogen. If we take as an approximation that the gas temperature is significantly higher than the grain temperature, we can use Eq. (2) to derive a relatively simple relationship between the gas temperature and the grain parameters:

$$T_G^{3/2} \propto \sigma_{gr}^{-1} n_{gr}^{-1} \quad (11)$$

As the mean grain cross section  $\sigma_{gr} \propto r_{gr}^2$ , and the number of grains  $n_{gr} \propto r_{gr}^{-3}$  this gives us a relationship between gas temperature and grain size:

$$T_G^{3/2} \propto r_{gr}^1 \quad (12)$$

As the Jeans mass within a cloud is proportional to  $T_G^{3/2} \rho_G^{-1/2}$  we find that the Jeans mass is proportional to  $r_{gr}^1$ . This result gives a clue to the possible causal link between

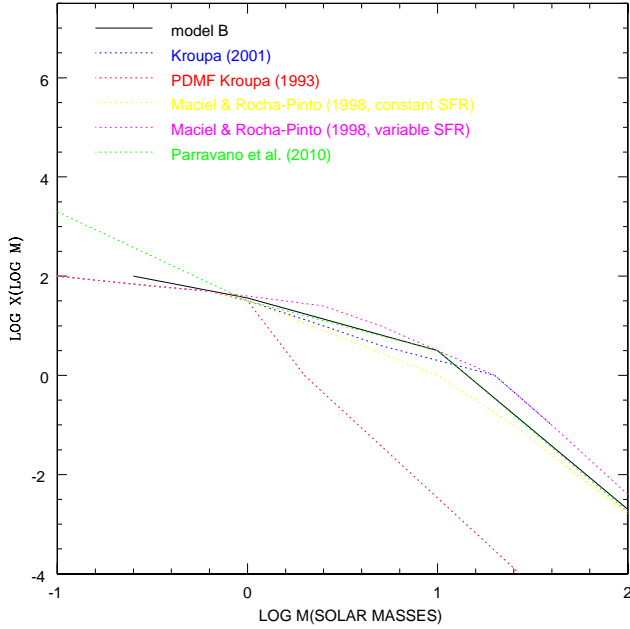


**Figure 5.** Prediction of our model B, which uses a theoretically derived molecular cloud mass function (Section 3.1.4) folded with the dust grain size function (Fig. 2), compared with the three chosen observational IMF's.

the characteristic dust grain size and the final characteristic stellar mass, which we show gives a stellar mass-grain radius relationship where  $M \propto r^{0.7}$ .

We can now go on to obtain an analytic approximation to the IMF, again assuming  $\text{IMF} \propto \text{GSDF} \times \text{MCGMF}$ , but now using an analytic fit to the data from CB10, in the form  $\text{GSDF} \propto r^{-3.6}$ , and taking MCGMF as derived in section 3.1.3. This formulation gives us:

$$\text{IMF} \propto M^{\alpha-4.6} \left[ e^{-\frac{M^{2\alpha}}{\eta}} + e^{-\frac{(M_G^\alpha - M^\alpha)^2}{\eta}} \right] \quad (13)$$

If we now use, following section 3.1.3,  $\eta \propto T_G$  and starting from Eq. (12), and the relation between the Jeans mass and  $r$ , we find:

$$\text{IMF} \propto M^{\alpha-4.6} \left[ e^{-\frac{M^{2\alpha-1}}{\eta'}} + e^{-\frac{(M_G^\alpha - M^\alpha)^2 M^{-1}}{\eta'}} \right] \quad (14)$$

where  $\alpha$ ,  $\eta$  and  $\eta'$  are constants.

#### 4 COMPARISON OF THE MODEL PREDICTIONS WITH OBSERVATIONS

We can see in Fig. 1 a comparison between the classical Salpeter's IMF and the PDMF of Kroupa et al. (1993) and also the IMF's of: Kroupa (2001), Maciel & Rocha-Pinto (1998) (in both cases, assuming constant SFR and variable SFR), and Parravano et al. (2011). In Figs. 4, 5 and 6 we can see the same data sample but compared with the predictions of our models presented in this paper (A, B, and C respectively). Our models A and C can fit reasonably well all the data between  $0.1 M_\odot$  and  $25 M_\odot$  except that of Parravano et al. (2011) for masses lower than  $1 M_\odot$  where the uncertainties in the observational data are largest. But

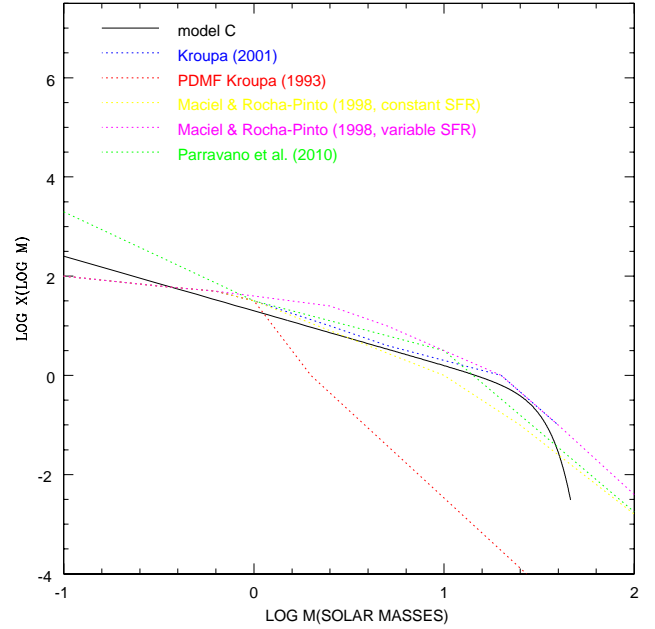


**Figure 6.** Prediction of our model C, in which the grain size distribution is derived from a model where the gas temperature is maintained close to equilibrium by radiation from the grains, which thereby influence the Jeans mass within the cloud, and hence the stellar mass. The IMF is determined using analytical expressions containing the cloud mass and grain size distributions. The observational IMF's are plotted for comparison.

the best fit is obtained for our model B where the GSDF is numerically derived and the MCGMF is derived analytically. We are not claiming here that we are in a position to decide finally which of the models gives the closest approach to the observations, particularly as the observations themselves are being continually revised. Nevertheless the introduction of the grain size dependence gives fits to the predicted IMF which are significant improvements on the use of the gas cloud mass function alone. We can see that the model A reproduces best the IMF derived by the later authors assuming a specific time-variable SFR produced from observational data of the chromospheric activity of local late type dwarfs. This agreement is in some sense model-dependent, because one of the underlying assumptions of the dust size distribution component of the model was the same time variation sequence in the SFR.

#### 5 CONCLUSIONS

This study offers prima facie evidence that there is a functional relationship between the characteristic masses of the stars at birth and the characteristic sizes of the dust grains which populate the molecular clouds giving rise to the stars. This relationship is superposed on a more conventionally accepted dependence of the stellar mass range on the placental molecular cloud mass range. The evidence comes from the superior fits to the observationally derived IMF's of the models in which the two distributions, the MCGMF and the DGSF are folded together, compared to models based

on the MCGMF alone. However we have also offered a semi-quantitative explanation based on scenarios describing the effects of the dust grains on the formation of the molecular clouds, and on the collapse of the cloud cores to form stars. The details of these processes include two specific properties of the grains which might appear strange. In their catalytic action leading to the formation of molecular from atomic hydrogen, the formation rates favour larger grains, because their effective surface areas are fractal, so that their surface to volume ratio increases with grain radius. The same grains acting to radiate away heat show the opposite behaviour; their outer surfaces from which radiation can escape are more effective for the smaller grains, because the ratio of the radiative surface to grain volume falls with grain radius. These effects are both present in the intervention of grains in the cloud forming process and the eventual star forming process, and we have taken them quantitatively into account when deriving the IMS's in all the models presented here. The relation of dust grain size  $r$  to stellar characteristic mass  $M$  can be summarized in the expression  $M \sim 25r^{0.7}$ , where  $M$  is in units of solar masses, and  $r$  is in microns. The dependence of the characteristic stellar mass on the mass of the placental molecular cloud  $M_C$  can also be parametrized, and takes the form  $M_C \sim 10^5 M$ .

## 6 ACKNOWLEDGMENTS

We are very grateful to the anonymous referee for the thorough comments which improved considerably the clarity in the structure of the article. This work was carried out with support from project AYA2007-67625-C02-01 of the Spanish Ministry of Science and Innovation, and from project P3/86 of the Instituto de Astrofísica de Canarias.

## REFERENCES

- Bigiel, F., Leroy, A., Walter, F., Brinks, E., de Blok, W. J. G., Madore, B., Thornley, M. D. 2008, *AJ*, 136, 2846
- Blitz, L., & Rosolowsky, E. 2004, *ApJ*, 612, L29
- Blitz, L., Rosolowsky, E. 2006, *ApJ*, 650, 933
- Bolatto, A. D., Leroy, A. K., Rosolowsky, E., Walter, F., Blitz, L. 2008, *ApJ*, 686, 948
- Casuso, E., & Beckman, J. E. 2002, *PASJ*, 54, 405
- Casuso, E., & Beckman, J. E. 2007, *ApJ*, 656, 897
- Casuso, E., & Beckman, J. E. 2010, *AJ*, 139, 1406
- Cazaux, S., & Spaans, M. 2004, *ApJ*, 611, 40
- Chandrasekhar, S. 1943, *Rev. Mod. Phys.*, 15, 1
- Clayton, G. C., Wolff, M. J., Sofia, U. J., Gordon, K. D., & Misselt, K. A. 2003, *ApJ*, 588, 871
- Elmegreen, B. G. 1989, *ApJ*, 338, 178
- Gould, R. J., & Salpeter, E. E. 1963, *ApJ*, 138, 393
- Jeans, J. H. 1902, *Philosophical Transactions of the Royal Society of London. Series A, Containing Papers of a Mathematical or Physical Character*, Vol. 199, 1
- Kennicutt, R. C., Jr., et al. 2007, *ApJ*, 671, 333
- Kim, S.-H., Martin, P. G., & Hendry, P. D. 1994, *ApJ*, 422, 164
- Kroupa, P., Tout, C. A., Gilmore, G. 1993, *MNRAS*, 262, 545
- Kroupa, P. 2001, *MNRAS*, 322, 231
- Maciel, W. J., & Rocha-Pinto, H. J. 1998, *MNRAS*, 299, 889
- Mutschke, H., Min, M., Tamanai, A. 2009, *A&A*, 504, 875
- Nozawa, T., Kozasa, T., Habe, A., Dwek, E., Umeda, H., tominaga, N., Maeda, K., Nomoto, K. 2007, *ApJ*, 666, 955
- Parravano, A., Mc Kee, Ch. F., Hollenbach, D. J. 2011, *ApJ*, 726, 27
- Rocha-Pinto, H. J., & Maciel, W. J. 1997, *MNRAS*, 289, 882
- Rocha-Pinto, H. J., Scalo, J., Maciel, W. J., Flynn, C. 2000, *A&A*, 358, 869
- Salpeter, E. 1955, *ApJ*, 121, 161
- Scalo, J. M., 1978, in Gehrels T. ed., *Protostars and Planets*, Univ. Arizona, p. 265
- Scalo, J. M., 1986, *Fund. Cosmic Phys.* 11,1
- Scalo, J. M. 1998, in *The Stellar Initial Mass Function*, ASP Conf. Ser. Vol. 142, Astron. Soc. San Francisco, p. 201
- Schaye, J. 2004, *ApJ*, 609, 667
- Schneider, R., Omukai, K., Inoue, A., Ferrara, A. 2006, *MNRAS*, 369, 1437
- Solomon, P. M., Rivolo, A. R., Barret, J., & Yahil, A. 1987, *ApJ*, 319, 730
- Tinsley, B. M., 1980, *Fund. Cosmic Phys.* 5, 287
- Vidali, G., Roser, J., Manico, G., Pirronello, V., Perets, H. B., Biham, O. 2005, *Journal of Physics Conf. Ser.* 6, 36
- Wong, T., Blitz, L. 2002, *ApJ*, 569, 157
- Weingartner, J. C., & Draine, B. T. 2001, *ApJ*, 548, 296
- Weingartner, J. C. 2006, *ApJ*, 647, 390

This paper has been typeset from a  $\text{\TeX}/\text{\LaTeX}$  file prepared by the author.